

## A broad band detector of Gravitational Waves: The dual torus

M.BONALDI<sup>1</sup>, M.CERDONIO<sup>2</sup>, L.CONTI<sup>2</sup>, M.PINARD<sup>3</sup>, G.A.PRODI<sup>4</sup>, L.TAFFARELLO<sup>5</sup>,  
J.P.ZENDRI<sup>5</sup>

<sup>1</sup> *Istituto di Fotonica e Nanotecnologie, ITC-CNR, Trento and I.N.F.N. Gruppo Coll. di Trento Sezione di Padova, I-38050 Povo, Trento, Italy.*

<sup>2</sup> *Department of Physics, University of Padova and I.N.F.N. Sezione di Padova, Via Marzolo 8, I-35131, Padova, Italy.*

<sup>3</sup> *Laboratoire Kastler Brossel, 4 Place Jussieu, F75252 Paris, France.*

<sup>4</sup> *Department of Physics, University of Trento and I.N.F.N Gruppo Coll. di Trento Sezione di Padova, I-38050 Povo, Trento, Italy.*

<sup>5</sup> *Istituto Nazionale di Fisica Nucleare I.N.F.N., Sezione di Padova, Via Marzolo 8, I-35131, Padova, Italy.*

The concept of a sensitive and broadband resonant gravitational wave detector is presented with reference to a dual torus. The detector is equipped with a readout which senses the quadrupolar vibrational modes while rejecting the contributions due to the other not gravitational wave sensitive modes. This feature lowers the total thermal noise and give a consistent reduction of the back-action noise. The sensitivity curve for a possible configuration is presented and compared to the one of the next generation of interferometers. For a Molybdenum dual detector the achievable sensitivity of  $\sim 3 \cdot 10^{-23} \text{ Hz}^{-1/2}$  in the frequency window between 2 kHz to 5 kHz is better or equal than the expected sensitivity of the up-graded interferometers.

### 1 Introduction

Astrophysical objects dominated by relativistic dynamic should produce gravitational waves (GW) with main frequency components in the ' $kHz$ ' region<sup>1</sup>. These GW carry information about the behavior of matter at extremely high density and about the gravitational interaction when strong non linear effects are expected. As the ' $kHz$ ' frequency region is the optimal one for the acoustic detectors we calculated the best sensitivity that they can achieve using a quantum noise limited readout and at the present state of material science. The detector design has been optimized to achieve wide bandwidth and thus a resonant readout can not be used. Indeed the resonant readout<sup>2</sup> produces a mechanical amplification which is useful to optimally match the GW sensitive resonators to the readout system; as a drawback the detector bandwidth is automatically limited and cannot be greater than  $\nu_0 \mu^{1/2}$  where  $\nu_0$  is the elastic body resonant frequency,  $\mu^{1/2} = (m_{tr}/M_{el})^{1/2}$  is the inverse of the mechanical amplification and  $M_{el}$  and  $m_{tr}$  are the sensitive elastic body and the resonant transducer equivalent mass respectively. Thus a broadband detector requires  $\mu \sim 1$  which makes the resonant transducer useless. The use of multimode transducer<sup>3</sup> should help to overcome this problem but at the price of an increase

of the detector complexity. Thus for our sensitivity analysis we assume that the detector is equipped with non resonant transducers. We considered a new detector geometry, which we call the dual detector, constituted by two nested elastic bodies. The centers of mass of the two bodies are designed to be coincident and thus only measurable effect of an incoming GW is the induced relative deformation of the elastic bodies. The implementations considered so far are the dual sphere, in which the elastic bodies have a spherical shape<sup>4,5</sup>, and the dual torus<sup>6</sup> where the external and internal bodies are respectively a hollow and a full cylinder. The advantage of the spherical geometry is the isotropic sensitivity while the second geometry can be realized more easily and host easily the wide area selective readout (see sect. 3). This paper is devoted to the description of the optimal design of the latter.

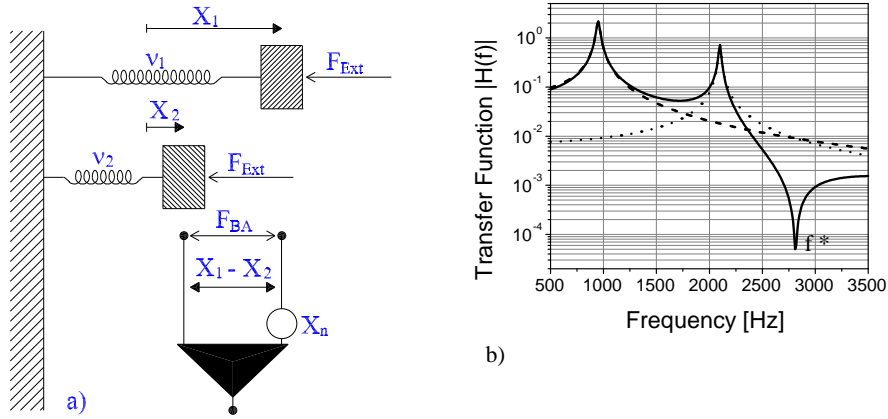


Figure 1: a) Lumped model of an acoustic dual detector. The gravitational equivalent force  $F_G$  acts on the two oscillators with approximately the same amplitude and sign. The measured quantity  $X_m$  is the difference of the two displacements  $X_1$  and  $X_2$ . The additive displacement noise generator  $X_n$  and the back-action force noise generator  $F_{BA}$  arising from the displacement amplifier are also shown. b) Absolute value of the transfer function  $H(f) = X(f)/F_G$  of the system: the dotted line and the dashed line are respectively the transfer function of the first and the second harmonic oscillator while the continuous line is the transfer function of the dual detector.

## 2 The one dimensional model

The usual description of a resonant detector in terms of an harmonic oscillator characterized by an effective mass, a resonant frequency and a mean displacement of its surface is inadequate when we have to deal with a broadband acoustic detector. The reason is that the off-resonance back-action and thermal noise of the non gravitationally excited acoustic modes give a non negligible contribution to the overall noise in the sensitive frequency window. Moreover the signal to noise maximization often requires to consider more than one GW sensitive internal mode. One possible solution to these problems is to use the modal expansion of the elastic body deformation. This method will be described in the next section while in this section we use the simplified lumped element model in order to understand our optimization procedure and some peculiarities of the dual detector. According to this model a dual detector is described by two harmonic oscillators and the relative displacement  $X_{meas} = X_1 - X_2$  is measured (see fig.1a)). Above the resonant frequency of the slow resonator and below the one of the fast one the displacements  $X_1$  and  $X_2$  induced by the gravitational wave equivalent force  $F_G$  are in opposite phase and thus the relative displacement  $X_{meas}$  is the sum of the absolute values of the displacement of each resonator. Thus, compared to the single resonator, the transfer function of a dual detector is enhanced between the two resonances; outside this frequency region the displacements are in phase the overall transfer function is reduced reaching a frequency (labelled  $f^*$  in figure 1b) where the measured

quantity  $X_{meas}$  is zero. Thus, compared to a single resonator detector, the dual detector has an higher sensitivity and bandwidth between the two resonances. Another particularity of the dual detector is the back-action effect cancellation around a frequency which we call  $f^{**}$ . Indeed the back-action force acts on both the oscillators with the same amplitude but opposite sign: in the frequency region between the resonances the back-action induced  $X_{meas}^{BA}$  is the difference of the absolute values of the back-action induced displacements  $X_1$  and  $X_2$ . When  $X_1(f) \sim X_2(f)$  (at  $f = f^{**}$ ) the back-action induced  $X_{meas}^{BA}$  is zero.

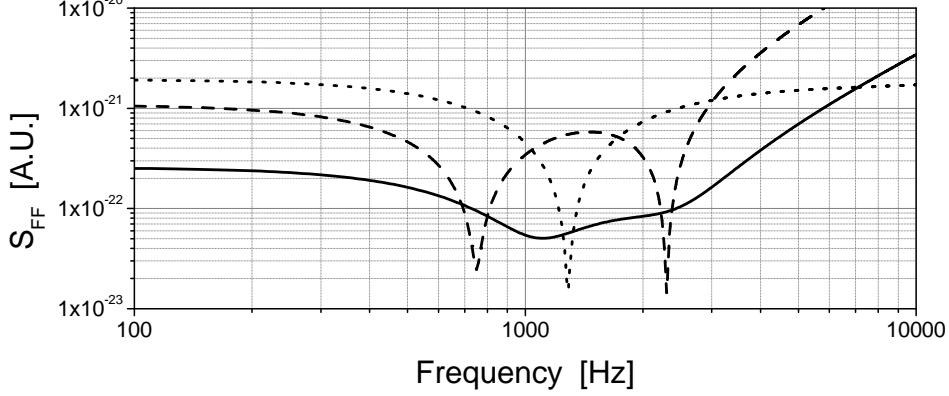


Figure 2: Input force power spectral density  $S_{FF}(\nu)$  for different values of the noise stiffness  $\mathcal{K}_n$ . The dashed, continuous and dotted lines correspond to values of  $\mathcal{K}_n$  increasing by a factor of 10

The dual detector optimization is optimized assuming that the displacement amplifier is dominated by the quantum noise according to

$$S_{F_{BA}F_{BA}}(\omega) \cdot S_{X_n X_n}(\omega) = \frac{\hbar^2}{2} \quad (1)$$

where  $S_{X_n X_n}(\omega)$  is the power spectral density of the amplifier's additive noise and  $S_{F_{BA}F_{BA}}(\omega)$  is the power spectral density of the amplifier's back-action noise force. This requirement still leaves the freedom of choosing the amplifier noise stiffness  $\mathcal{K}_n$ :

$$\mathcal{K}_n(\omega) \equiv \sqrt{\frac{S_{F_{BA}F_{BA}}(\omega)}{S_{X_n X_n}(\omega)}} \quad (2)$$

A large value of  $\mathcal{K}_n$  corresponds to a detector dominated by the back-action force and thus the noise curve is expected to have a deep minimum where the back-action effect is cancelled out (i.e at the frequency  $f^{**}$ ) see fig.2. On the contrary, when  $\mathcal{K}_n$  is low, the dominant effect is the additive amplifier noise and thus the sensitivity is maximized at the detector quadrupolar resonances where transfer function is high enough to overcome the amplifier additive noise. Finally, an intermediate value of  $\mathcal{K}_n$  produces a broad band noise curve (continuous line in fig.2). This latest condition is the one to be achieved when choosing the  $\mathcal{K}_n$  that optimizes the dual detector sensitivity over a broad frequency range.

### 3 The modal expansion and the off-resonance noise reduction

The elastic body strain  $\vec{u}(\vec{r}, t)$  can be written as:

$$\vec{u}(\vec{r}, t) = \sum_m b_n(t) \vec{w}_m(\vec{r}) \quad (3)$$

where  $\vec{w}_m(\vec{r})$  are the solutions of the eigenvalue problem of the considered body<sup>8</sup> and  $b_m(t)$  are the time dependent coefficients which have a Fourier transform amplitude  $b_m(\omega)$  that satisfies the linear equation:

$$-\omega^2 b_m(\omega) + \omega_m^2 (1 + i\phi(\omega)) b_m(\omega) = \frac{F(\omega)}{\rho} \int dV \vec{G}(\vec{r}) \cdot \vec{w}_m(\vec{r}) \quad (4)$$

Here  $\omega_m$  is the eigenvalue of  $m$ -th mode,  $\phi(\omega)$  a frequency dependent phenomenological coefficient introduced to describe the material structural damping and  $F(\omega) \cdot \vec{G}(\vec{r})$  the Fourier transform of the force field applied to the elastic body. The latter could be generated by a gravitational signal or by a noise force like the thermal and the back-action forces. According to General Relativity the GW induced force field is quadrupolar and thus only the modes  $\vec{w}_m(\vec{r})$  with a relevant quadrupolar component can be excited by the incoming GW. On the contrary in general the field that describes the perturbation induced by a noise force has a not quadrupolar symmetry: the noise induced coefficients  $b_m$  can be significantly different from zero for any  $m$  of the expansion (3). Thus the simplified model used in the previous section, which considers only the GW induced quadrupolar modes, overestimates the signal to noise ratio because it neglects all the modes that are not excited by a gravitational wave but that contribute to the overall noise. In order to reduce this systematic error we calculate the sensitivity of the dual torus summing eq.3) up to  $m=50$ . An higher mode number is not required as we already reach saturation<sup>6</sup>.

In order to reduce the unwanted noise contribution of the non GW sensitive modes a careful choice of the surface where the elastic body deformation is averaged over needs to be done. Indeed in general the measured displacement  $X_{meas}$  is defined as:

$$X_{meas}(t) = \int_S dS \vec{P}(\vec{r}) \cdot \vec{u}(\vec{r}, t) = \sum_m b_m(t) \int_S dS \vec{P}(\vec{r}) \cdot \vec{w}_m(\vec{r}) \quad (5)$$

where  $\vec{P}(\vec{r})$  is a weight function and the second equality arises from eq.(3). If the weight function is uniform and constant over a large area, the contribution of the low wavelength (high frequency) modes to the summation (5) becomes negligible as the product  $\vec{P}(\vec{r}) \cdot \vec{w}_m(\vec{r})$  averages to zero when integrated over the elastic body surface  $S$ . The cancellation effect scales quadratically with the surface integral: it can be demonstrated<sup>8</sup> that the back-action and the thermal noise spatial distributions  $\vec{G}(\vec{r})$  are equal to the weight function  $\vec{P}(\vec{r})$  and thus, according to eq.(4), also the  $b_m$  coefficient amplitudes are proportional to the surface integral of  $\vec{P}(\vec{r}) \cdot \vec{w}_m(\vec{r})$ . The large area readout is very efficient in rejecting the high frequency modes but is practically inefficient for the modes with wavelength comparable or larger than the sensed area. To reject the noise contribution coming from these modes we use a weight function with a quadrupolar symmetry: we refer to it as the 'selective readout'. This particular choice maximizes the contribution of the GW excited quadrupolar modes to  $X_{meas}$  as the overlapping between  $\vec{P}(\vec{r})$  and  $\vec{w}_n(\vec{r})$  is maximal; for the non quadrupolar modes the sign of the product  $\vec{P}(\vec{r}) \cdot \vec{w}_n(\vec{r})$  oscillates and thus the surface integral of eq.(5) is strongly depressed. In practice it is difficult to implement a pure quadrupolar weight function and thus an approximated quadrupolar function has to be considered. As a possible implementation we consider the dual torus equipped with a capacitive readout (see fig.3a)). Here the quadrupolar selective readout is obtained combining the measured relative displacements of the two tori  $X_i$  averaged over 4 large areas rotated by 90° with respect to each other. To be more precise the measured displacement is defined as  $X_{meas} = X_1 + X_3 - X_2 - X_4$  where the sign of each  $X_i$  is determined by the electric bias field polarity (fig.3a)). The efficiency of the selective readout to reject the noise contribution of the non quadrupolar modes is evident from fig.3c) where we compare the noise curve of a dual torus equipped with a selective readout (fig.3a)) to that with a non selective readout (fig.3b)).

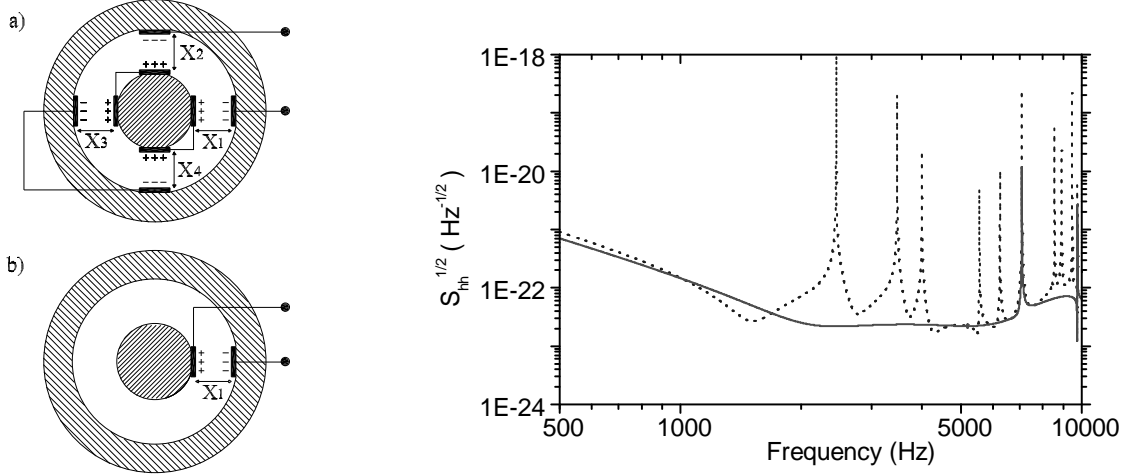


Figure 3: a) Dual torus with selective readout: the measured displacement is  $X_{meas} = X_1 - X_2 + X_3 - X_4$ . b) Dual torus with not selective readout: here  $X_{meas} = X_1$ . c) Equivalent strain power spectral density for both cases: the dotted line is for the non selective readout while the continuous line for the selective readout. For the calculation we use a molybdenum internal cylinder 0.5 m in diameter and an external torus with internal diameter of 0.52 m and external diameter of 0.94 m. The fraction of circumference covered by the readout is approximately 20 % which is a compromise to have a large area and a selective readout.

#### 4 Results and discussion

The eigenfunctions of a hollow cylinder with infinite height can be written in terms of a linear superimposition of Bessel functions. Using this analytical solution we calculated the sensitivity of the dual torus with the help of a numerical code for the estimation of the surface integrals and the solution of the eigenvalue problem. As the sensitivity curve scales with this product  $\rho v_s^4$ , where  $v_s$  is the material sound velocity, the best detector material should maximize this value. Moreover the candidate material should have also a high mechanical quality factor  $Q$  and a high thermal conductivity which are necessary to approach the required value of  $Q/T \sim 10^8 K^{-1}$ : this value makes the thermal noise contribution lower or equal to the amplifier noise. We choose Molybdenum (Mo) as the material because it has already demonstrated the required  $Q/T$ <sup>9</sup> and has a high  $\rho v_s^4$ ; it is also available in large samples at relatively low cost. The calculated sensitivity curve for a Molybdenum (Mo) dual torus detector is plotted in figure 4.

The noise curve of fig.4 is obtained using a quantum limited readout and an optimized value of the stiffness constant  $\mathcal{K}_n \sim 10^{11} N/m$ . A displacement readout which satisfies these two requirements is presently not available. To check how far we are from this ideal configuration and which parameters have to be improved we consider two different kinds of readout technology: the capacitive transducer read by a dc-SQUID and the optical transducer<sup>11</sup> which are presently under development by our group. The energy resolution achieved so far with the SQUID amplifier is about  $30 \hbar$ <sup>7</sup> not too far from the quantum limited value. The noise stiffness which scales with the square of the transducer bias field and this is presently limited by the vacuum breakdown field to about  $10^7 V/m$ . Using the above parameters the present best value of the noise stiffness is about  $\mathcal{K}_n \sim 10^7$ . Although this value seems to be dramatically lower than the required one, it should be considered that in the literature a value of the breakdown field of the order of  $10^9 V/m$  has been reported<sup>10</sup> over small areas; thus if we are able to reproduce this value over extended surfaces a value of  $\mathcal{K}_n$  near the ideal one could be approached. For the optical transducer the situation is different: the value  $\mathcal{K}_n \sim 10^{11} N/m$  can be achieved using a laser input power of about 1W and a Fabry-Perot cavity finesse of about  $10^6$ , already obtained values. In this case the problems are related to the implementation of the wide area sensing and to the extraction

of the heat caused by the laser power dissipated on the mirrors. To solve the first problem a folded Fabry-Perot cavity<sup>12</sup> has been proposed.

We can conclude that the feasibility study of the dual detector require a strong effort to improve the present readout sensitivity. For this reason in figure 4 we also draw the expected sensitivity curve of the advanced version of the ground based interferometers. It is evident that the potential sensitivity of both kinds of detector is complementary.

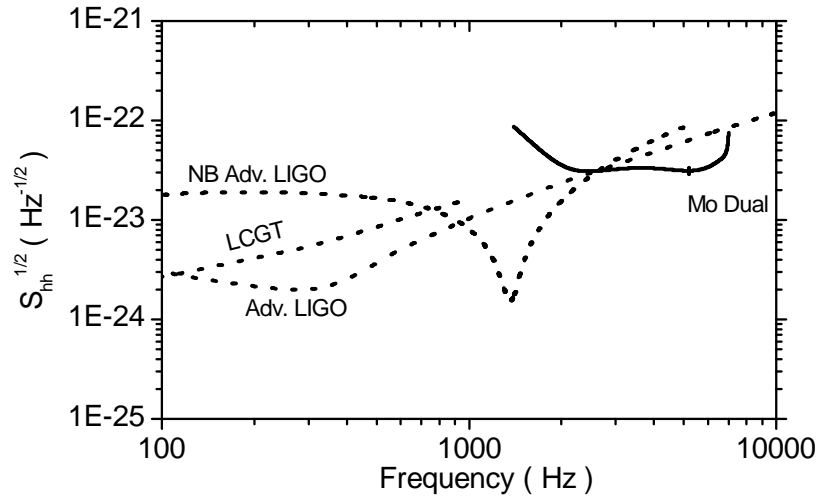


Figure 4: Predicted equivalent sensitivity curve for a Molybdenum dual torus detectors. The others curves are those of the next generation of interferometers.

## 5 References

1. see for instance V.Ferrari and N. Andersson in these proceedings.
2. H.J.Paik, *Jour. of Appl. Phys.*, **47**, 1168 (1976).
3. J.-P.Richard, *Phys. Rev. Lett.*, **52**, 165 (1984).
4. M.Cerdonio *et al*, *Phys. Rev. Lett.*, **87**, 031101 (2001).
5. T.Briant *et al*, *Phys. Rev.*, **D67**, 102005 (2003).
6. M. Bonaldi, arXiv:gr-qc/0302012
7. R.Mezzena *et al*, *Rev. Sci. Instrum.* **72** 3694 (2001).
8. M.Bonaldi *et al*, *Proc. of 15th SIGRAV Conference on Gen. Rel.*, Monte Porzio Catone, Roma, Italy (2002) in press.
9. W.Duffy, *J. Appl. Phys.* **72**, 5628 (1992)
10. W.T.Diamond, *J. Vac. Sci. Tech* **A16**, 707 (1998).
11. L.Conti *et al*, *Jour. Appl. Phys.* **93**, 3589 (2003).
12. F.Marin in these proceedings or *Phys. Lett.* **A 309**, 15 (2003).